DOI: 10.1002/ejoc.200600610

Crystal Structures of Conformationally Locked Cyclitols: An Analysis of Hydrogen-Bonded Architectures and their Implications in Crystal Engineering

Goverdhan Mehta,*[a] Saikat Sen,[a] and Senaiar S. Ramesh[a]

Keywords: Crystal engineering / Conformational locking / Cyclitols / Fused-ring systems / Hydrogen bonds

A qualitative study has been carried out on selected polycyclitols to evaluate the potential of conformational locking of hydroxy groups in lending predictability to the O–H···O hydrogen-bonding network observed in the crystal structures of such compounds. The polycyclitols employed in this study are conformationally locked with all the hydroxy groups destined to be axial owing to the *trans* ring fusion(s) in the polycyclic carbon framework. The consequent formation of intramolecular O–H···O hydrogen bonds between the 1,3-*syn* diaxial hydroxy groups now permits any packing pattern in the polycyclitols to be described in terms of a small group of intramolecularly bonded molecular motifs linked to their respective neighbors by four O–H···O bonds. By using this model and the results of CSD analyses of polyols as a guide, the O–H···O hydrogen-bonded packing motifs most likely to be observed in the crystal structure of each polycyclitol were proposed and compared with those obtained experimentally.

Introduction

Crystal engineering is being increasingly recognized as the supramolecular equivalent of organic synthesis.[1,2] The rational design of the crystal structure of an organic compound depends heavily on the predictability of the molecular self-organization through noncovalent interactions. Though sufficiently weaker than covalent bonds, these supramolecular interactions are directional enough to cooperatively assemble molecules in a manner that can be reasonably predicted.[1,2] Among the variety of intermolecular interactions that have been recognized in the crystal structures of organic compounds, the O–H···O hydrogen bond is among the most commonly encountered, thoroughly studied and extensively documented noncovalent bond.[3] In fact, O–H···O hydrogen bonds appear in a large number of supramolecular synthons that are routinely utilized in crystal engineering.[1,2]

Polyhydroxylated compounds, which include many biologically important molecules such as sugars and inositols, have long been used as model systems for the systematic study of O–H···O hydrogen bonds.[3a,b,d] The hydrogen-bonding patterns in the crystal structures of these compounds, as determined by neutron diffraction and high-precision X-ray analyses, have been incisively studied and extensively reported. Not surprisingly, the large database of these accurately determined crystal structures has, over the years, constantly stimulated research into formulating a set of empirical rules that govern the packing of polyols in the solid state. An attempt in this direction led Jeffrey and Saenger to point out that hydrogen bonding in carbohydrates follows certain patterns that are based on two primary concepts:[3a,3b] a) maximization of the total number of hydrogen bonds per molecule using as many donor/acceptor oxygen atoms as possible and b) maximization of the cooperativity by forming as many finite and infinite chains of hydrogen bonds as possible.

The former of the two concepts highlights a fundamental feature of any self-assembling process, striving to optimize all the interactions available at its disposal. Not surprisingly, it has been found to hold good in the crystal structures of not only carbohydrates, but also a number of other mono- and polyhydroxylated species as well. The second concept, namely the occurrence of cooperative O–H···O hydrogen-bonding chains, has however been shown recently by Taylor and Macrae to be strongly dependent on not only the number of OH groups in a particular polyhydroxylated species, but also the steric environment (the degree of substitution) around each hydroxy functionality.[4] Based on a CSD survey encompassing 144 monoalcohol (C_nH_mOH) and 101 dialcohol [$C_nH_m(OH)_2$] crystal structures, the authors were further able to lay down certain empirical rules governing the O–H···O hydrogen-bonding motif preferred in a particular mono- or dialcohol packing assembly. The pivotal role played by steric effects in the crystal packing of a polyol was again underlined in a contemporary CSD study on *vic*-diols by Brock, wherein it was observed that the extent of O–H···O bond formation itself depends on the degree of substitution of the *vic*-diol, an $R^2_2(10)$ dimer being the preferred motif in fully hydrogen-bonded crystal

[a] Department of Organic Chemistry, Indian Institute of Science, Bangalore 560012, India
Fax: +91-80-2360-0936
E-mail: gm@orgchem.iisc.ernet.in

structures.[5] Bishop and co-workers also concluded that molecular bulk or shape is important in dictating the choice of hydrogen-bonded motifs adopted by alcohols from a separate CSD analysis of the occurrence of ladder-like supramolecular architectures in certain diols.[6]

Though based on investigations carried out on specific classes of alcohols, it is reasonable to believe that the generalizations put forth in these CSD analyses can be used as a preliminary guide to understanding the selection of O–H···O hydrogen-bonding motifs observed in crystal structures of polyols structurally and constitutionally dissimilar to the coterie studied. In keeping with our ongoing interest in the study of the supramolecular assemblies adopted by conformationally constrained polycyclitols,[7,8] we were specifically interested in utilizing these rules as the basis for proposing the various possible modes in which polyols such as **1**, **2** and **3** are likely to pack in the solid state (Figure 1).

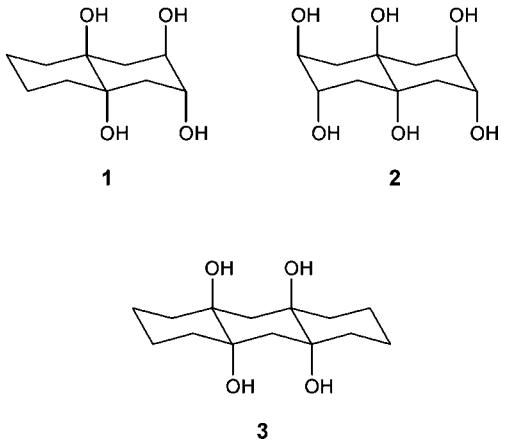

Figure 1. The conformationally locked polycyclitols used in this study.

In each of the three molecules **1**–**3**, the hydroxy groups are destined, owing to the *trans* ring fusion(s), to be locked in an axial conformation[9] and are thus favorably positioned (on account of their 1,3-*syn* diaxial relationship) to participate in intramolecular O–H···O hydrogen bonding. Hence, the packing pattern that is eventually observed in the fully hydrogen-bonded structures of **1**–**3** will essentially be determined by the manner in which intramolecularly hydrogen-bonded molecular motifs **4**–**8** (Figure 2) choose to be linked to its neighbors through the four intermolecular O–H···O hydrogen bonds. We intended to proceed along similar lines to build O–H···O hydrogen-bonded molecular ensembles from the motifs **4**–**8**, then use the results of the CSD analyses described above[4–6] to propose the most likely packing modes in the crystal structures of **1**–**3** and compare the results with those obtained experimentally. The principal goal of the study was to examine the influence of conformational locking in facilitating the prediction of O–H···O hydrogen-bonding patterns in polycyclitols and this paper details our efforts along these lines.

Results and Discussion

Synthesis of the Polycyclitols 1–3

The polycyclitols **1**–**3** were synthesized starting from readily available aromatic precursors (tetralin, naphthalene and anthracene, respectively) by sequential epoxidation and acid-catalyzed ring-opening of their Birch reduction products (Scheme 1, Scheme 2 and Scheme 3).[10] Thus, the unsaturated *trans*-diols **9** and **10**, obtained from tetralin and naphthalene, respectively, as described previously,[9a,11] were subjected to epoxidation with MCPBA to afford the monoepoxide **11** and the *anti*-diepoxide **12**, respectively. The stereoselective formation of **12**, whose structure was unambiguously assigned by single-crystal X-ray diffraction analysis, can be attributed to the formation of a pre-reaction hydrogen-bonded complex between two molecules of the peracid and the *trans* hydroxy groups in **10**.[12] This evidently leads to *anti*-selective oxygen delivery from MCPBA to the two double bonds in **10** (Figure 3). The desired polycyclitols

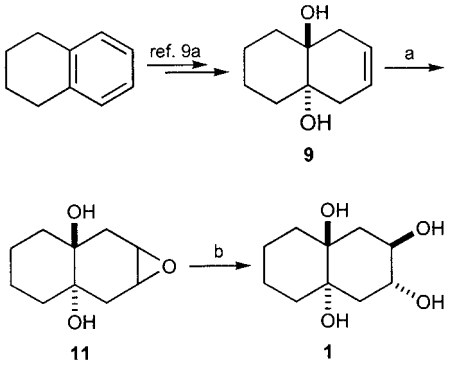

Scheme 1. Reagents and conditions: a) MCPBA, CH_2Cl_2, 0 °C → room temp., 30 min, 85%; b) 10% AcOH, room temp., 4 h, 90%. MCPBA: *m*-chloroperbenzoic acid.

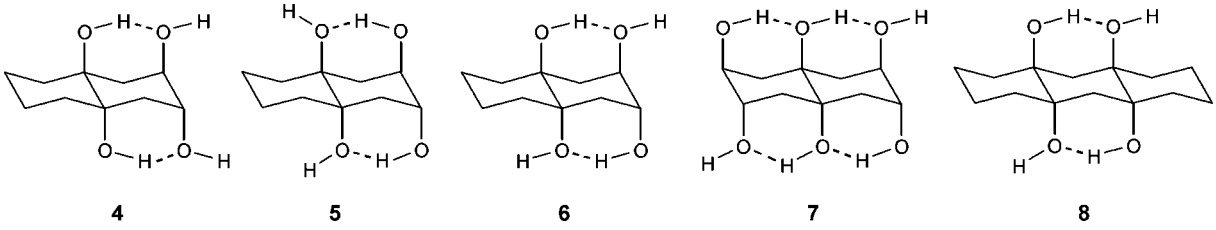

Figure 2. The conformationally locked, intramolecularly O–H···O hydrogen-bonded molecular motifs.

1 and **2** were obtained as the sole products upon mild acid-catalyzed hydrolysis of the oxirane functionalities in **11** and **12**, respectively (Scheme 1 and Scheme 2).

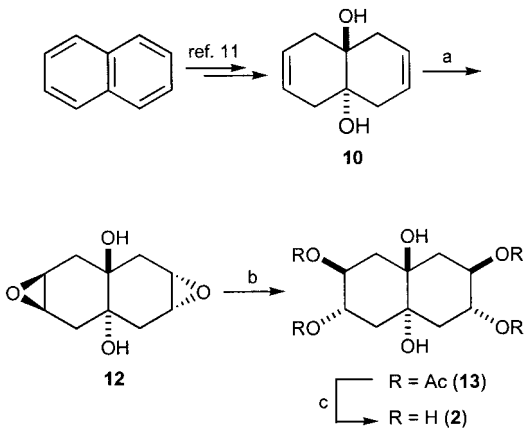

Scheme 2. Reagents and conditions: a) MCPBA, CH_2Cl_2, 0 °C → room temp., 3 h, 87%; b) i) *p*TSA, moist DCM, room temp.; ii) Ac_2O, pyridine, room temp., 20 h (65% over two steps); c) NaOMe, MeOH, 0 °C, 16 h, quant.

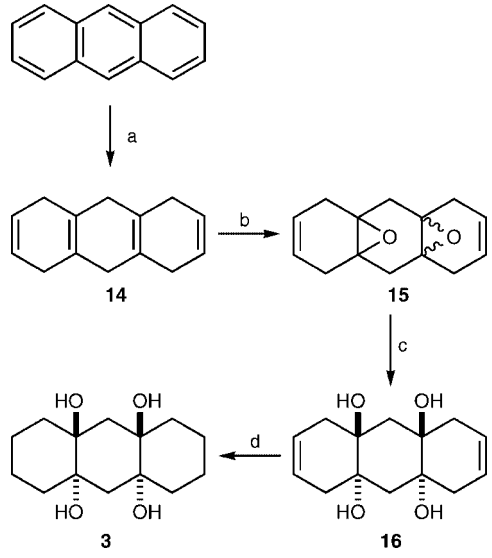

Scheme 3. Reagents and conditions: a) Na, liq. NH_3, EtOH, THF, –78 °C, 12 h, 80%; b) MCPBA, CH_2Cl_2, –20 °C, 5 min, *syn*/*anti* = 10:3, 89% overall yield; c) 10% AcOH (aq), 50–60 °C, 6 h, 95%; d) 5% Pd-C, H_2, MeOH, 1 h, 95%.

To synthesize **3**, anthracene-derived tricyclic tetraene **14**[13] was subjected to regioselective epoxidation of the internal double bonds to furnish a mixture (10:3) of *syn* and *anti* diastereomers of the diepoxide **15**.[14] Subsequent hydrolysis of the mixture of diepoxides **15** afforded a single unsaturated tetrol **16**,[14c] which on catalytic hydrogenation furnished the required tetrol **3**.

Note that cyclohexanetetrol, obtained upon acid- or base-catalyzed epoxide ring-opening of both *syn*- and *anti*-1,4-cyclohexane dioxide, displays solely a *trans-anti-trans* configuration of the OH groups, rather than the *trans-syn-trans* configuration observed in **1**–**3**.[15] The mechanism proposed by Craig et al. for the nucleophilic ring-opening reactions of 1,4-cyclohexane dioxide suggests that the configuration of the functional groups observed in the products arises from an initial axial attack of the nucleophile to open the first epoxide ring, followed by the inversion of the diaxially substituted epoxide intermediate to the diequatorial isomer, which then suffers a second axial nucleophilic attack to furnish the product.[15a] The methodology followed in the synthesis of the polycyclitols **1**–**3** thus utilizes the stability and conformational rigidity of the *trans*-decalin framework to establish the desired all-axial stereochemistry of the *trans*-hydroxy groups in the epoxide ring-opening steps.

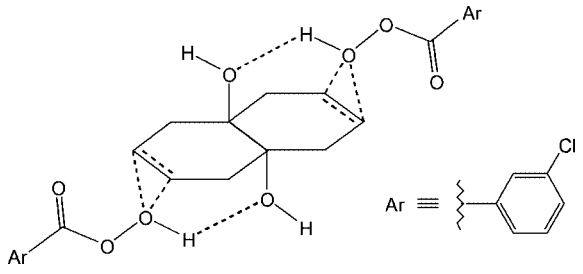

Figure 3. Proposed hydrogen-bonded complex between MCPBA and the diol **10**.

The Most Probable O–H···O Hydrogen-Bonded Packing Motifs in Crystal Structures of the Polycyclitols 1–3

In order to propose the O–H···O hydrogen-bonded packing motif most likely to be observed in crystal structures of the polycyclitols **1**–**3**, it was necessary to identify first the most likely ways by which an intramolecularly bonded molecular motif **4**–**8** may be bonded to its immediate neighbors by the four intermolecular O–H···O hydrogen bonds. Hence, among the large variety of packing patterns that may be speculated for the polycyclitols **1**–**3**, we decided to limit our choices to the well-documented preferences of hydrogen-bonding motifs in solid-state aggregates of polyhydroxylated molecules (vide supra).[3a,4–6] In other words, it was assumed that in the crystal structures of **1**–**3**, the formation of infinite –OH···OH– chains would be preferred if steric factors permit, intermolecular –OH···OH– rings being the next favored hydrogen-bonding motif.[4] However, even with this restriction, it was still possible to conceive of a significantly large number of packing patterns for the polycyclitols **1**–**3** by varying Z' (the number of molecules per asymmetric unit) and the symmetry elements relating a molecular motif to its immediate neighbors.

In such a case, if one assumes, as for example in the packing of the tetrol **1**, $Z' \leq 1$ and the highest possible rotation symmetry in the crystal is limited to a two-fold symmetry, following the space group statistics for 2°-3° dialcohols by Taylor and Macrae, it is possible to recognize 12 modes of molecular packing, all embodying infinite co-

operative –OH···OH– chains between the intramolecularly hydrogen-bonded 2°-3° OH pairs (Figure 4).[4] Each of these four packing modes can, in turn, be constructed from pairs of molecular motifs **4**–**6** related by two-fold, mirror, inversion, 2_1 screw and/or glide operations.

However, on closer inspection, it becomes apparent that the modes of molecular assembly depicted in parts f–l in Figure 4 (those shown in Figure 4, j–l in particular) will lead to unfavorable spatial segregation of the interacting cyclohexanetetrol moieties, on account of the steric bulk of the intervening cyclohexane rings, and therefore render untenable the formation of infinite intermolecular O–H···O hydrogen bonds. Therefore it would appear that the five patterns of molecular packing envisaged in Figure 4 (a–e) may be the ones most likely to be observed in the supramolecular assembly of the tetrol **1**. It is pertinent to emphasize at this point that supramolecular assemblies of **1** incorporating the packing modes shown in Figure 4 (f–l) may still

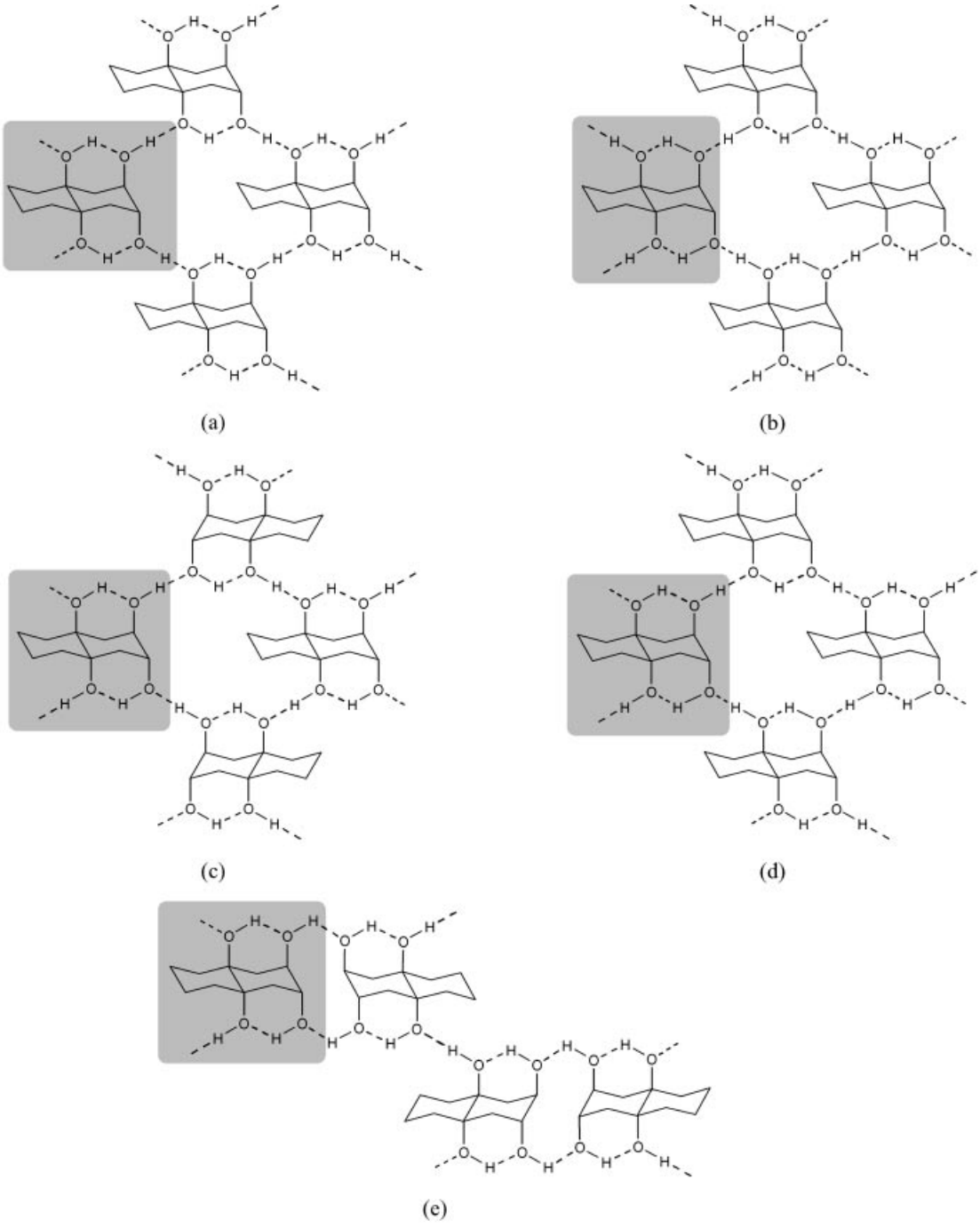

Figure 4. The packing modes proposed for the tetrol **1** (assuming $Z' \leq 1$ and limiting the highest possible rotation symmetry in the crystal to a two-fold symmetry). All of them incorporate infinite cooperative –OH···OH– chains between the intramolecularly hydrogen-bonded 2°-3° OH pairs. The respective molecular motifs **4**–**6** have been highlighted with a gray background.

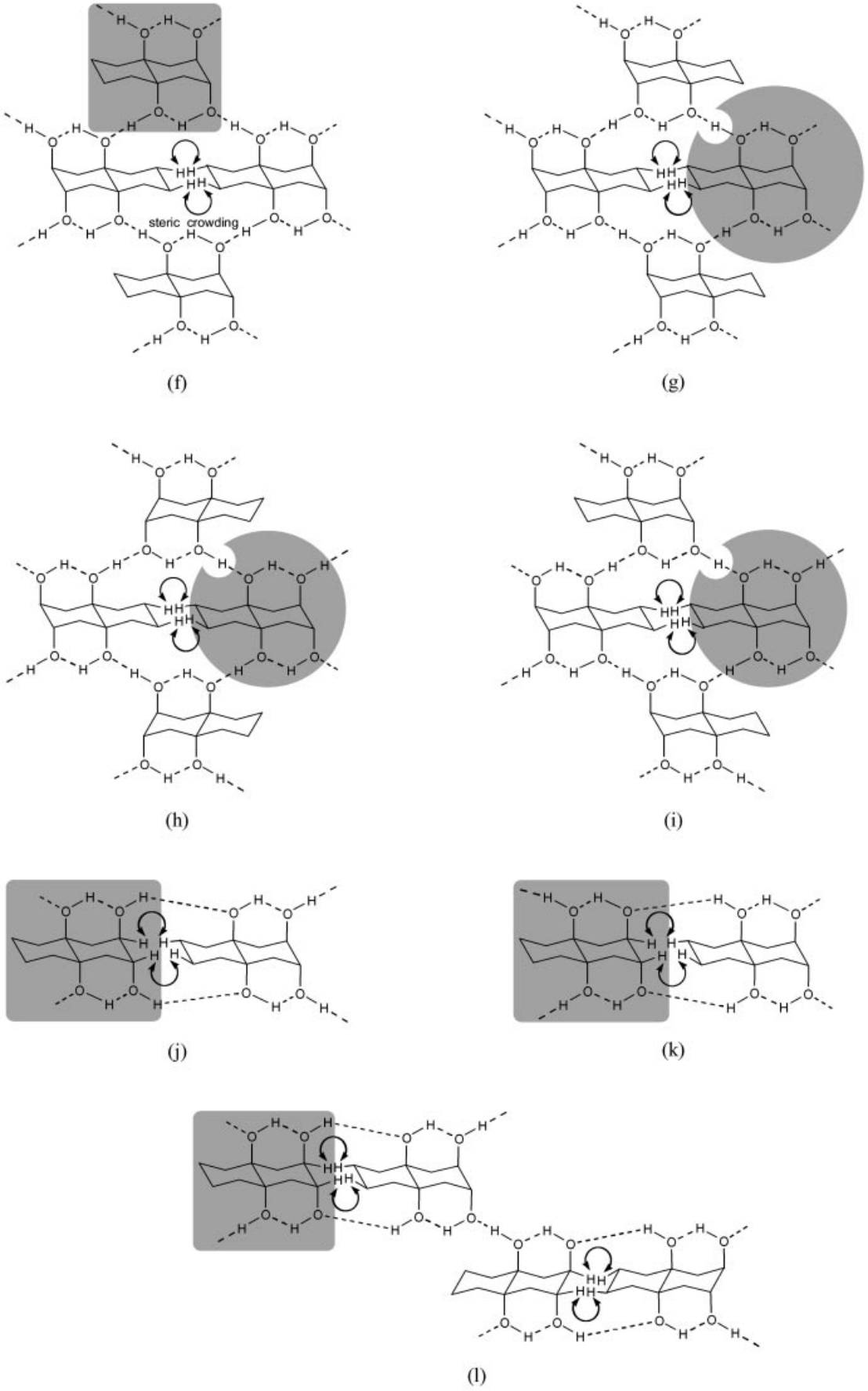

Figure 4. *(continued)*.

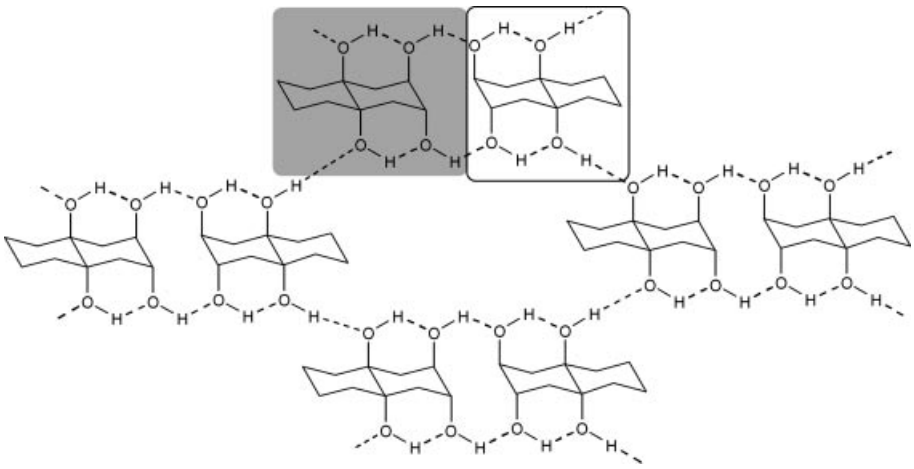

Figure 5. The packing mode proposed for the tetrol **1** assuming $Z' = 2$. The two crystallographically independent molecules constitute the molecular motifs **4** (gray background) and **5** (encircled).

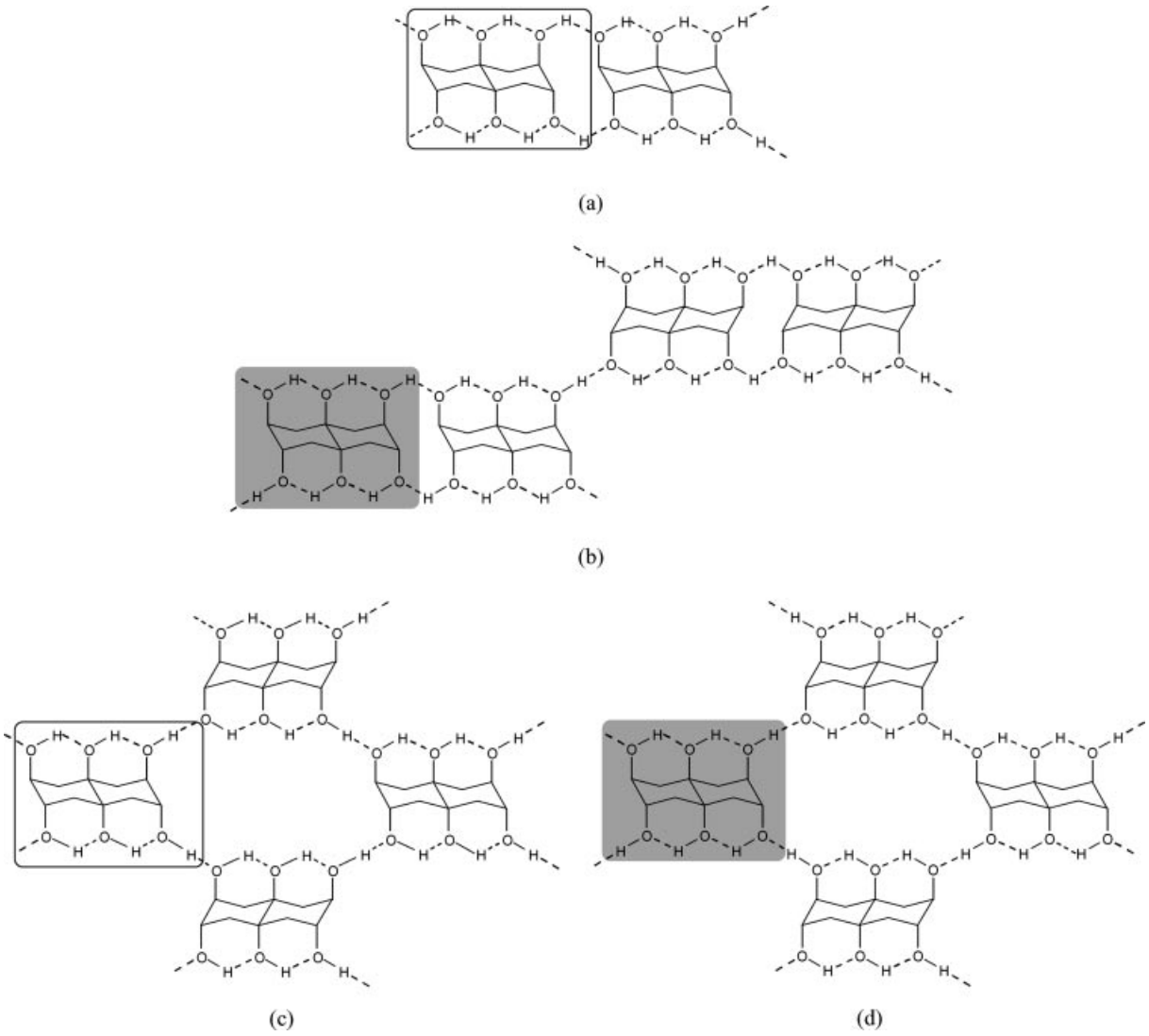

Figure 6. The four packing modes proposed for the hexol **2** (assuming $Z' \leq 1$ and limiting the highest possible rotation symmetry in the crystal to a two-fold symmetry). All of them incorporate infinite cooperative –OH···OH– chains. The centric motif **7** has been highlighted with a gray background, while the noncentric one has been encircled.

be realized if one relaxes the constraint on Z' and the allowed space group symmetry. For example, by allowing two molecules of **1** to reside in the asymmetric unit (i.e. $Z' = 2$), one may possibly tune the spatial relationship among the crystallographically independent molecules suitably enough to offset the steric constraints on the intermolecular O–H···O hydrogen bonding encountered in such molecular packing (Figure 5).

Assuming identical constraints on Z' and crystal symmetry, one may propose, by following almost the same line of arguments as put forward in the case of **1**, that each intramolecularly hydrogen-bonded molecule of **2** can be linked to its nearest neighbors according to the four different O–H···O hydrogen-bonding schemes depicted in Figure 6 (a–d). As shown in the case of **1** above (Figure 4), all four hydrogen-bonding patterns proposed for **2** follow the same trend observed by Jeffrey and Saenger in as much as they maximize not only the number of O–H···O bonds,[3a,3b] but also the hydrogen-bond cooperativity owing to the formation infinite –OH···OH– chains. However, it is well known that an achiral molecule like the C_{2h} symmetric hexol **2** would prefer to crystallize in a centrosymmetric space group[16] and usually occupy, according to a CSD study by Brock and Dunitz, the crystallographic inversion centers ($Z' = ½$) in such a case.[17] Hence, the centrosymmetric molecular packings (Figure 6, b and d) generated from the centric molecular motif **7** would appear to be among the four depicted in Figure 6 more likely to be observed in the crystal structure of the hexol **2**.

In comparison to the polycyclitols **1** and **2**, the four hydroxy groups in the achiral C_{2h} symmetric tetrol **3** are tertiary. The space group and Z' statistics in the CSD study by Taylor and Macrae reveal that while 89% of the 3°-3° dialcohols studied crystallized in the top 15 space groups, 82% of them adopted structures with $Z' = 1$. In addition, among the 10 3°-3° diols that adopted packing motifs involving intramolecular O–H···O hydrogen bonds, five formed –OH···OH– chains, two preferred rings and three favored isolated O–H···O hydrogen bonds.[4] In the light of these observations, one may be tempted to extend to the C_{2h} symmetric tetrol **3** the same line of arguments as adopted for the isosymmetric hexol **2**, subject to identical constraints on the highest-allowed crystal symmetry and Z' (= ½), and propose a centrosymmetric model of molecular packing, as shown in Figure 7. The supramolecular aggregate can be generated through suitable symmetry operations on the centric molecular motif **8** and can, in principle, result in the formation of infinite –OH···OH– chains among the intramolecularly bonded pairs of tertiary hydroxy groups.

However, as argued in the case of **1**, the steric hindrance caused by the intervening cyclohexane rings in the molecular assembly depicted in Figure 7 will lead to weakening of the intermolecular O–H···O hydrogen bonds between the interacting cyclohexanetetrol moieties in **3** (Figure 7). As noted in the case of **1** and quite applicable to **2**, viable supramolecular assemblies of the tetrol **3**, embodying –OH···OH– chains, may still be generated from the molecu-

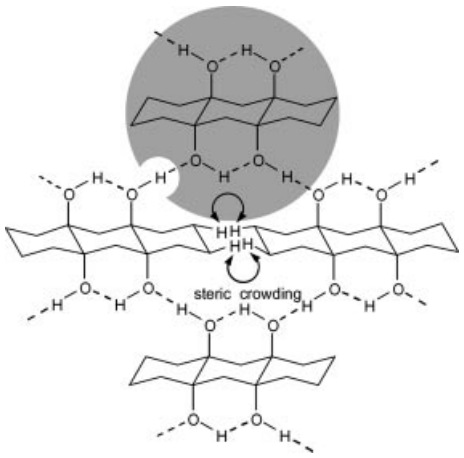

Figure 7. A centrosymmetric packing mode proposed for the tetrol **3** (assuming $Z' = ½$ and limiting the highest possible rotation symmetry in the crystal to a two-fold symmetry) that is capable of incorporating, in principle, infinite cooperative –OH···OH– chains. The centric molecular motif **8** has been highlighted with a gray background.

lar motif **8** if one relaxes the constraint on Z' and the allowed space group symmetry. As an illustration, one may follow the example of the packing pattern shown in Figure 5 and possibly overcome the steric constraints to intermolecular O–H···O hydrogen bonding encountered in the molecular ensemble depicted in Figure 7 by allowing molecules of **3** to occupy two sets of inversion centers (i.e. $Z' = 2 \times ½ = 1$) instead of one (Figure 8).

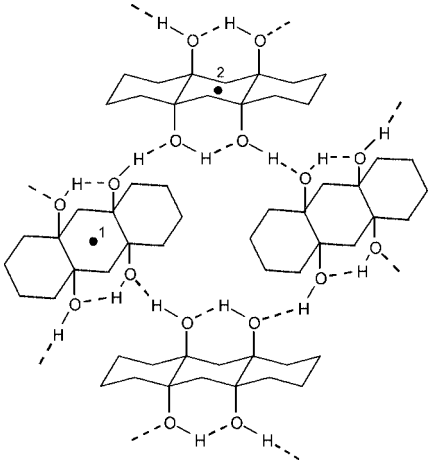

Figure 8. A centrosymmetric packing mode proposed for the tetrol **3** (assuming $Z' = 2 \times ½$ and limiting the highest possible rotation symmetry in the crystal to a two-fold symmetry) that is capable of incorporating infinite cooperative –OH···OH– chains. The centric molecular motif **8** occupies two sets of inversion centers (marked with a dot, and labeled 1 and 2).

It is also possible for the self-assembling process to overcome the steric inhibition to molecular packing in **3** by opting for the formation of –OH···OH– rings, as a second alternative, through a "broadside" approach of the interacting cyclohexanetetrol moieties. In such a case, even with the constraint of **3** preferring to crystallize in a low symmetry centrosymmetric space group with $Z' = ½$, it is easily pos-

sible to conceive of a molecular packing, as depicted in Figure 9, generated from translationally related molecular motifs **7** linked to each other through four intermolecular O–H···O hydrogen bonds. Interestingly, this proposed packing pattern, consisting of alternate regions of organic cycles (defined by the carbocyclic framework) and centrosymmetric $(OH)_4$ rings, is quite reminiscent of the step-ladder architectures adopted by certain classes of dialcohols.[6]

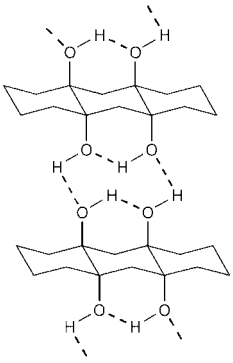

Figure 9. A centrosymmetric packing mode proposed for the tetrol **3** (assuming $Z' = ½$ and limiting the highest possible rotation symmetry in the crystal to a two-fold symmetry), incorporating –OH···OH– rings.

X-ray Crystallographic Studies on the Polycyclitols 1–3

Crystals of the polycyclitols **1**–**3** suitable for single-crystal X-ray crystallography were grown under ambient temperature and pressure from their solutions in 1:1:2 dry methanol/ethanol/ethyl acetate. None of the polycyclitols showed any polymorphic or pseudopolymorphic modification under the crystallization conditions described. The details of the packing patterns in the polycyclitols **1**–**3**, as gleaned from an analysis of their respective crystal data (see Table 4), are discussed below.

Crystal Structure of the Polycyclitol 1

The crystal structure of the bicyclic C_2 symmetric tetrol **1** (Figure 10) was solved and refined in the noncentrosymmetric orthorhombic space group *Fdd2* ($Z = 16$).[18] The two pairs of 1,3-*syn* diaxial hydroxy groups participate in intramolecular hydrogen bonding in a manner exhibited by

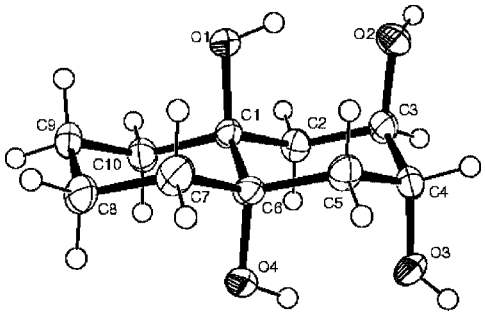

Figure 10. ORTEP diagram of **1** with the atomic numbering scheme for the asymmetric unit. Displacement ellipsoids for non-hydrogen atoms have been drawn at the 50% probability level.

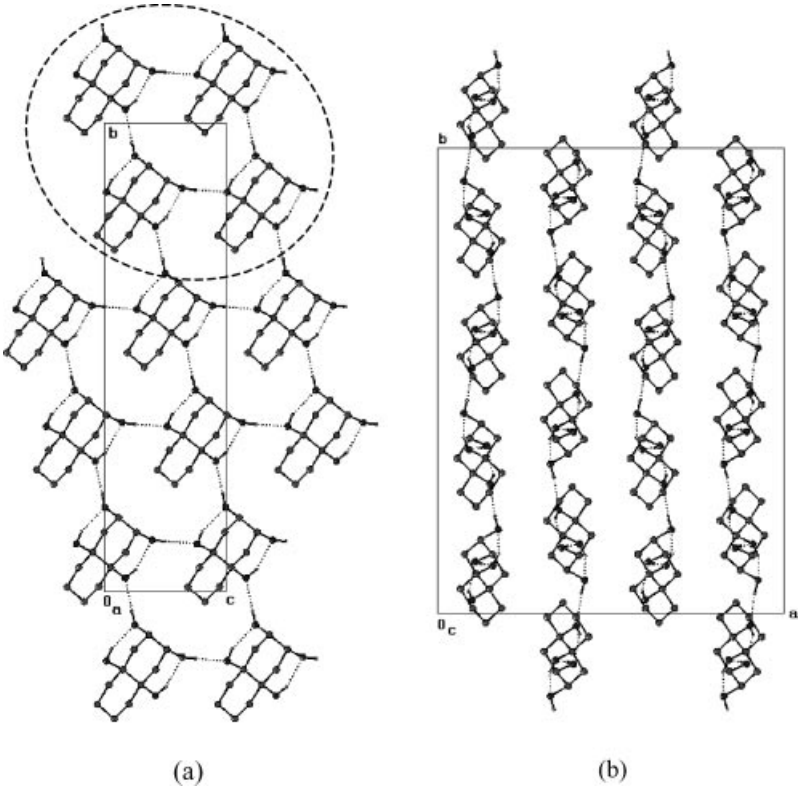

(a) (b)

Figure 11. Crystal packing in the tetrol **1**, showing details of the hydrogen-bonded tapes, viewed along a) the *a* axis and b) the *c* axis. The hydrogen atoms connected to the carbon atoms have been omitted for clarity. A portion of the packing diagram in (a) has been encircled to show its resemblance to part a of Figure 4. The packing diagram in (b) shows the typical layered appearance of the supramolecular assembly.

the molecular motif **4**. Four intermolecular O–H···O hydrogen bonds, involving O2–O4 and O3–O1, link each tetrol molecule to its nearest neighbors to form hydrogen-bonded tapes perpendicular to the (100) direction (part a of Figure 11, Table 1).

Table 1. Hydrogen bond geometry in **1**.[a]

D–H···A	*r*(D–H) [Å]	*r*(H···A) [Å]	*r*(D···A) [Å]	D–H···A [°]
O1–H1O···O2^{i}	0.82	1.98	2.710(2)	148
O2–H2O···O4^{ii}	0.82	1.99	2.810(2)	175
O3–H3O···O1^{iii}	0.82	2.01	2.836(2)	177
O4–H4O···O3^{i}	0.82	2.01	2.735(3)	147

[a] Symmetry codes: i) x, y, z; ii) $-x+¼$, $y+¼$, $z+¼$; iii) x, y, $z-1$.

These hydrogen-bonded tapes are translated along the *a* axis and are held together solely by weak van der Waals interactions between the cyclohexane rings, so that when viewed perpendicular to the *ab* plane, the packing pattern assumes a layered structure reminiscent of graphite (Figure 11, b).

Crystal Structure of the Polycyclitol 2

The bicyclic C_{2h} symmetric hexol **2** (Figure 12, a) packed in the centrosymmetric monoclinic space group $P2_1/n$ (Z = 2) with the molecular inversion centers coinciding with the crystallographic centers of symmetry at (0, 0, 0) and (½, ½, ½). Like **1**, the intramolecularly hydrogen-bonded molecules of the hexol **2** participate in four intermolecular O–H···O hydrogen bonds involving O2 and O3 to form O–H···O hydrogen-bonded tapes perpendicular to the (101) direction (part b of Figure 12, Table 2).

Table 2. Hydrogen bond geometry in **2**.[a]

D–H···A	*r*(D–H) [Å]	*r*(H···A) [Å]	*r*(D···A) [Å]	D–H···A [°]
O1–H1O···O2^{i}	0.82	2.00	2.730 (1)	149
O2–H2O···O3^{ii}	0.82	1.95	2.756 (2)	169
O3–H3O···O1^{iii}	0.82	2.04	2.718 (1)	140

[a] Symmetry codes: i) x, y, z; ii) $x+½$, $-y+½$, $z+½$; iii) $-x+1$, $-y+1$, $-z+1$.

Crystal Structure of the Polycyclitol 3

The tricyclic C_{2h} symmetric tetrol **3** (Figure 13, a) crystallized in the centrosymmetric triclinic space group $P\bar{1}$ (Z = 1) with the molecular inversion centers coinciding with the crystallographic centers of symmetry at (½, 0, ½). Unlike **1** and **2**, the O–H···O hydrogen bonds in the tetrol **3** form a cyclic $(OH)_4$ motif (a quadrilateral four-membered homodromic hydrogen-bonding cycle),[3b] so that the molecules are linked by four intermolecular O–H···O hydrogen bonds to form chains growing parallel to the *a* axis (Figure 13, b, Table 3). The translationally related molecular chains are held in space solely by weak van der Waals interactions between the cyclohexane rings (Figure 13, b).

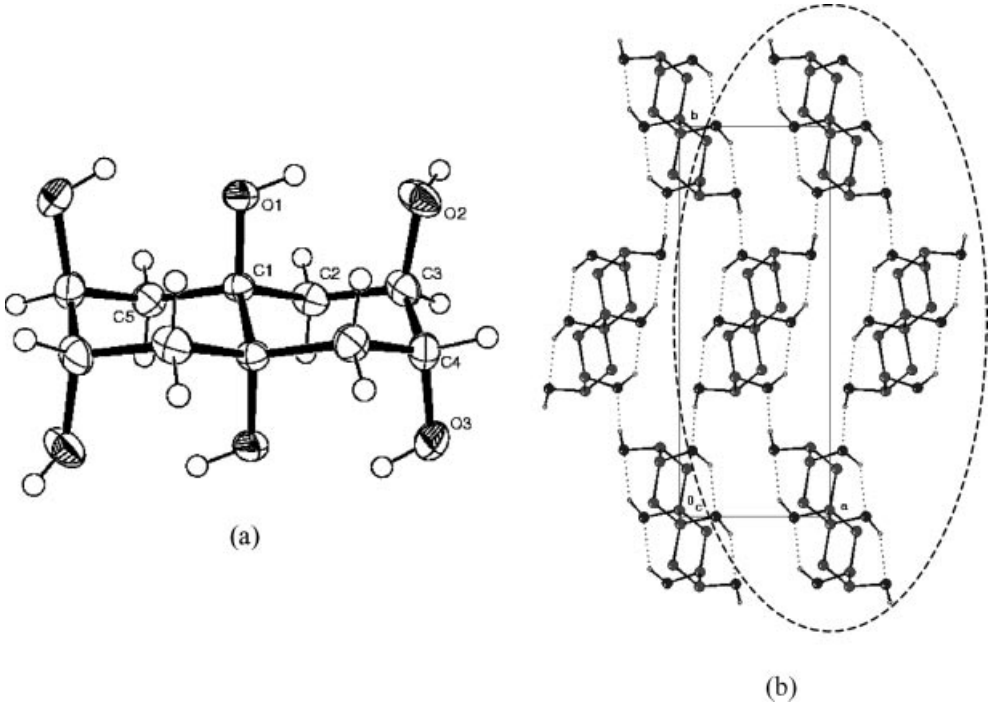

Figure 12. a) ORTEP diagram of **2** with the atomic numbering scheme for the asymmetric unit. Displacement ellipsoids for non-hydrogen atoms have been drawn at the 50% probability level. b) Crystal packing in the hexol **2** viewed along the *c* axis. The hydrogen atoms connected to the carbon atoms have been omitted for clarity. A portion of the packing diagram in (b) has been encircled to show its resemblance to part d in Figure 6.

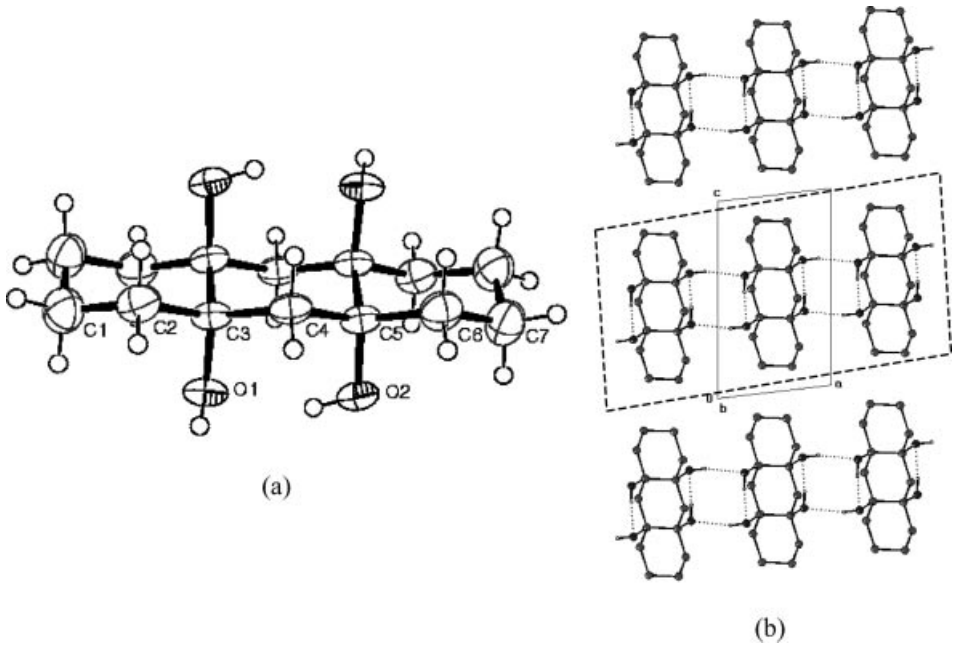

Figure 13. a) The ORTEP diagram of **3** with the atomic numbering scheme for the asymmetric unit. Displacement ellipsoids for non-hydrogen atoms have been drawn at the 50% probability level. b) Crystal packing in the hexol **3** viewed along the *b* axis. The hydrogen atoms connected to the carbon atoms have been omitted for clarity. A portion of the packing diagram in (b) has been encircled to show its resemblance to Figure 9.

Table 3. Hydrogen bond geometry in **3**.[a]

D–H···A	*r*(D–H) [Å]	*r*(H···A) [Å]	*r*(D···A) [Å]	D–H···A [°]
O1–H1···O2^{i}	0.82	2.01	2.814 (3)	167
O2–H2···O1^{ii}	0.82	1.94	2.670 (3)	148

[a] Symmetry codes: i) $-x, -y, -z+1$; ii) x, y, z.

Comparison of the Experimentally Obtained Packing Motifs with Those Proposed for 1, 2 and 3

A close examination of the crystal structures of the polycyclitols **1**–**3** (Figure 11, a, Figure 12, b, Figure 13, b) revealed that the O–H···O hydrogen-bonding pattern observed experimentally for a particular polyol resembled very closely one of those proposed as most probable for it (Figure 4, a–e, Figure 6, b,d and Figure 9). As assumed on the basis of space group and Z' statistics for dialcohols, none of the polycyclitols **1**–**3** crystallized in unusually high-symmetry space groups or adopted crystal structures with $Z' > 1$.[4] The C_{2h} symmetric polyols **2** and **3** showed the usual preference of achiral molecules for centrosymmetric space groups and indeed occupied one set of inversion centers, as proposed on the basis of observations by Brock and Dunitz.[16,17] The formation of infinite –OH···OH– chains in the supramolecular assembly of **1** and **2** and the adoption of O–H···O rings in the crystal structure of **3** as an alternative to the sterically unfavorable chain motif are in consonance with the order of preference of the basic hydrogen-bonding motifs reported for mono- and dialcohols by Taylor and Macrae.[4] Note that the formation of –OH···OH– rings in the crystal structure of the tetrol **3** can also be attributed to the self-assembling process, striving to optimize not only the strong and directional O–H···O hydrogen bonds, but also the weak and isotropic van der Waals interactions by increasing the area of contact between the parallel cyclohexane rings.

Conclusions

As a corollary to the view put forth by Jeffrey in his seminal review "Crystallographic Studies of Carbohydrates",[3a] polyhydroxylated molecules, such as the ones chosen in this study, constitute one of the simplest systems for the analysis of hydrogen bonding because they have only one functional group, namely the hydroxy group, which functions as both donor and acceptor of hydrogen bonds in the molecule. On the contrary, prediction of the mode of molecular association through intermolecular O–H···O hydrogen-bonds in such molecules becomes a difficult proposition owing to the orientational flexibility of the C–OH groups. Proposing the hydrogen-bonded architecture in polyols with little or no constraints to the internal degrees of freedom proves to be even more complicated as the final spatial disposition of the hydroxy groups realized in the crystal structure of such molecules is often largely determined by the crystal packing itself. In this study, we have therefore attempted to analyze the influence of the conformational locking of hydroxy groups in lending greater predictability to the hydrogen-bonded packing motifs adopted by polyhydroxylated molecules.

For the polycyclitols **1**–**3** chosen for this analysis, conformational locking and the consequent intramolecular O–H···O hydrogen bonding between the 1,3-*syn* diaxial OH

groups allowed any packing pattern in **1**–**3** to be described in terms of a handful of intramolecularly hydrogen-bonded molecular motifs **4**–**8**. Thus, despite considering fully hydrogen-bonded structures of a tetrol or hexol, it was possible, in combination with the well-documented results of CSD analyses of polyols, to narrow down the number of packing motifs most likely to be observed in the polycyclitols **1**–**3**. This, coupled with the fact that the experimentally observed packing motifs corroborate well those proposed for **1**–**3**, provides room for speculation on the possibility of conformational locking facilitating prediction of hydrogen bonding in molecules having not only hydroxy groups, but also other functionalities (such as NH_2 and COOH). Hence the results presented in this study are significant from the standpoint of crystal engineering and may provide leads for the identification of new supramolecular synthons in conformationally constrained systems.

Experimental Section

General: Melting points were recorded with a Büchi B-540 apparatus and are uncorrected. Infrared spectra were recorded with a JASCO FT-IR 410 spectrometer. ^{1}H and ^{13}C NMR spectra were recorded with a JEOL JNM-LA 300 spectrometer. Chemical shifts are reported with respect to tetramethylsilane (Me_4Si) as the internal standard (for ^{1}H NMR) and the central line (δ = 77.0 ppm) of $CDCl_3$ (for ^{13}C NMR). The chemical shifts are expressed in parts per million (ppm, δ values) downfield from Me_4Si. The standard abbreviations s, d, t, q and m refer to singlet, doublet, triplet, quartet and multiplet, respectively. Coupling constant (J), whenever discernible, are reported in Hz. Both low-resolution (LRMS) and high-resolution mass spectra (HRMS) were recorded with a Q-TOF Micromass mass spectrometer. Reactions were monitored by thin-layer chromatography (TLC) performed either on (10 × 5 cm) glass plates or on microscopic slides coated with silca gel G (Acme) containing 13% calcium sulfate as a binder. Visualization of the spots on the TLC plates was achieved by exposure to iodine vapor, by using UV radiation or by spraying with either ethanolic vanillin or 30% methanol-sulfuric acid solution and heating the plates at 120 °C. Commercial silica gel (Acme, 100–200 mesh particle size) was used for column chromatography. The columns were usually eluted with ethyl acetate/hexane mixtures. All solvent extracts were washed with water and brine, dried with anhydrous sodium sulfate and then concentrated under reduced pressure on a rotary evaporator unless specified otherwise. Yields reported are isolated yields of materials judged homogeneous by TLC and NMR spectroscopy.

(1a*R,2a*S**,6a*S**,7a*S**)-Perhydronaphtho[2,3-*b*]oxirene-2a,6a-diol (11):** MCPBA (734 mg, 2.976 mmol, 70% purity) was added to a solution of the *trans*-diol **9** (500 mg, 2.976 mmol) in dichloromethane (10 mL) at 0 °C. The reaction was stirred at room temperature for 30 min and then quenched by addition of a saturated solution of sodium sulfite in water. The product was extracted with dichloromethane (3 × 20 mL); the combined extracts were washed successively with saturated sodium hydrogen carbonate solution and brine, and then dried with anhydrous sodium sulfate. Removal of the solvent and subsequent purification by column chromatography with 25% ethyl acetate/hexane afforded the monoepoxide **11** (465 mg, 85%). ^{1}H NMR (300 MHz, $CDCl_3$): δ = 3.56 (s, 2 H, OH), 3.42–3.39 (m, 1 H), 3.33–3.31 (m, 1 H), 2.21 (½ABq, J = 17 Hz, 1 H), 2.17 (½ABq, J = 15 Hz, 1 H), 1.96–1.77 (m, 3 H), 1.72–1.35 (m, 7 H) ppm. ^{13}C NMR (75 MHz, $CDCl_3$): δ = 70.9 (2 C), 54.7, 51.6, 36.3, 34.6, 34.1, 32.8, 21.1, 20.1 ppm. LRMS (ES, 70 eV): m/z = 207 [M + Na]$^+$. HRMS (ES): calcd. for $C_{10}H_{16}O_3Na$ [M + Na]$^+$ 207.0997; found 207.1002.

(2*R,3*R**,4a*S**,8a*S**)-Perhydro-2,3,4a,8a-naphthalenetetrol (1):** A suspension of the monoepoxide **11** (200 mg, 1.087 mmol) in acetic acid (10% solution in water, 5 mL) was stirred at room temperature for 4 h. The volatiles were then removed under vacuum and subsequent purification of the residue by column chromatography using 50% ethyl acetate/hexane furnished the required tetrol **1** (198 mg, 90%). M.p. 171.1–171.8 °C (dec.). IR (KBr): $\tilde{\nu}$ = 3310 cm^{-1}. ^{1}H NMR (300 MHz, D_2O): δ = 3.88 (s, 2 H), 1.96 (½ABq, J = 15 Hz, 2 H), 1.62–1.53 (m, 2 H), 1.43 (½ABq, J = 15 Hz, 2 H), 1.40–1.22 (m, 6 H) ppm. ^{13}C NMR (75 MHz, $CDCl_3$): δ = 74.9 (2 C), 71.3 (2 C), 33.9 (2 C), 33.5 (2 C), 20.1 (2 C) ppm. LRMS (ES, 70 eV): m/z = 225 [M + Na]$^+$. HRMS (ES): calcd. for $C_{10}H_{18}O_4Na$ [M + Na]$^+$: 225.1103; found 225.1099.

Perhydrooxireno[2′,3′:6,7]naphtho[2,3-*b*]oxirene-2a,5a-diol (12): A solution of MCPBA (1.485 g, 6.024 mmol, 70% purity) in dichloromethane (5 mL) was added dropwise to a solution of the *trans*-diol **10** (500 mg, 3.012 mmol) in dichloromethane (5 mL) at 0 °C. The white suspension thus formed was stirred at room temperature for 3 h and then quenched by addition of a saturated solution of sodium sulfite in water. The product was extracted with dichloromethane (3 × 30 mL); the combined extracts were washed successively with saturated sodium hydrogen carbonate solution and brine, and dried with anhydrous sodium sulfate. Removal of the solvent and subsequent purification by column chromatography with 35% ethyl acetate/hexane afforded the diepoxide **12** (519 mg, 87%). IR (KBr): $\tilde{\nu}$ = 3487 cm^{-1}. ^{1}H NMR (300 MHz, $CDCl_3$): δ = 3.61 (s, 2 H, OH), 3.40–3.38 (m, 2 H), 3.31–3.28 (m, 2 H), 2.14 (d of ABq, J = 15, 2 Hz, 8 H) ppm. ^{13}C NMR (75 MHz, $CDCl_3$): δ = 69.7 (2 C), 54.4 (2 C), 51.1 (2 C), 35.5 (2 C), 32.4 (2 C) ppm. LRMS (ES, 70 eV): m/z = 221 [M + Na]$^+$. HRMS (ES): calcd. for $C_{10}H_{14}O_4Na$ [M + Na]$^+$ 221.0785; found 221.0790.

Perhydro-2,3,4a,6,7,8a-naphthalenehexol (2): A solution of the diepoxide **12** (200 mg, 1.010 mmol) in moist dichloromethane (10 mL) was stirred at room temperature in the presence of a catalytic amount of *p*TSA. After completion of the reaction, the volatiles were removed under vacuum and the residue, thus obtained, was acetylated at room temperature in presence of acetic anhydride and pyridine. The reaction takes 20 h to complete as indicated by TLC analysis. At the end of this period, the reaction was quenched with water and the product extracted with dichloromethane (3 × 20 mL). The combined extracts were washed with saturated sodium hydrogen carbonate solution and brine, and dried with anhydrous sodium sulfate. Removal of the solvent and subsequent purification by column chromatography with 50% ethyl acetate/hexane afforded the tetraacetate **13** (264 mg, 65% over two steps) as a colorless solid. IR (KBr): $\tilde{\nu}$ = 3585, 1732 cm^{-1}. ^{1}H NMR (300 MHz, $CDCl_3$): δ = 5.07 (s, 4 H), 3.14 (s, 2 H), 2.27 (½ABq, J = 15 Hz, 4 H), 2.08 (s, 12 H), 1.77 (½ABq, J = 15 Hz, 4 H) ppm. ^{13}C NMR (75 MHz, $CDCl_3$): δ = 169.2 (4 C), 72.16 (2 C), 69.9 (4 C), 33.2 (4 C), 21.2 (4 C) ppm. LRMS (ES, 70 eV): m/z = 425 [M + Na]$^+$. HRMS (ES): calcd. for $C_{18}H_{26}O_{10}Na$ [M + Na]$^+$ 425.1424; found 425.1429.

The pure tetraacetate **13** (150 mg, 0.373 mmol) thus obtained was dissolved in dry methanol (1 mL) and sodium methoxide (85 mg, 1.567 mmol) was added to the resulting solution. The reaction mix-

ture was stirred at room temperature under dry nitrogen for 16 h. The solvent was then completely removed under vacuum and the residue dissolved in a minimum volume of deionized water. The solution was passed through a short column of pretreated DOWEX® 50W ion-exchange resin (8–200 mesh, acidic cation) and washed with deionized water. The aqueous solution of the product thus obtained was concentrated under vacuum to obtain the hexol **2** (87 mg) in quantitative yield. M.p. 248.5–249.1 °C (dec.). IR (KBr): $\tilde{\nu}$ = 3585, 1732 cm^{-1}. ^{1}H NMR (300 MHz, D_2O): δ = 3.84 (s, 4 H), 3.08 (½ABq, J = 15 Hz, 4 H), 1.54 (½ABq, J = 15 Hz, 4 H) ppm. ^{13}C NMR (75 MHz, D_2O): δ = 75.9 (2 C), 71.3 (4 C), 33.5 (4 C) ppm. LRMS (ES, 70 eV): m/z = 257 [M + Na]$^+$. HRMS (ES): calcd. for $C_{10}H_{18}O_6Na$ [M + Na]$^+$ 257.1001; found 257.0995.

1,4,5,8,9,10-Hexahydroanthracene (14): Compound **14** was synthesized following an adapted procedure of Birch et al.[13a] Anthracene (1 g, 0.565 mmol) was dissolved in dry THF (80 mL) and dry ethanol (25 mL, 0.430 mol). The mixture was added to liquid ammonia (80 mL) and the vigorously stirred suspension of anthracene was reduced with sodium (2.6 g, 0.113 mol) at –78 °C. The mixture was stirred for 12 h after which ammonia was allowed to evaporate. Water (50 mL) was then added to dissolve the inorganic salts completely. The product was extracted with diethyl ether (3 × 50 mL), and the combined ether extracts washed with brine and dried with anhydrous sodium sulfate. Removal of the solvent and subsequent column chromatography through neutral alumina using a 2% EtOAc/petroleum ether mixture afforded the product as a colorless, crystalline solid (800 mg, 80%). M.p. 146.5–147.0 °C (ref.[13c] 147.5–148.5 °C). ^{1}H NMR (300 MHz, $CDCl_3$): δ = 5.49 (s, 4 H), 2.57 (s, 8 H), 2.43 (s, 4 H) ppm.

4a,9a:8a,10a-Diepoxy-1,4,4a,5,8,8a,9,9a,10,10a-decahydroanthracene (15): A solution of MCPBA (1.340 g, 5.434 mmol, 70% purity) in dichloromethane (40 mL) was added dropwise to a solution of hexahydroanthracene **14** (500 mg, 2.717 mmol) in dichloromethane (20 mL) cooled to –30 °C. The reaction was stirred at the same temperature for 5 min and was then quenched with a saturated solution of sodium hydrogen carbonate. The product was extracted with dichloromethane (3 × 20 mL); the combined extracts were washed with saturated sodium hydrogen carbonate solution and brine, and dried with anhydrous sodium sulfate. Removal of the solvent afforded the crude diepoxide **15** as a stereoisomeric mixture that can be used directly in the preparation of the tetrol **16**. However separation of the isomeric diepoxides by column chromatography presents no great difficulty as their polarity varies widely. Usual chromatographic separation of the crude mixture with 30% ethyl acetate/hexane yielded successively the *anti*-(120 mg) and *syn*-diepoxides (400 mg) in 89% overall yield.

***anti*-Diepoxide:** M.p. 186.9–187.6 °C (dec.). ^{1}H NMR (300 MHz, $CDCl_3$): δ = 5.40 (s, 4 H), 2.49 (½ABq, J = 18 Hz, 4 H), 2.28 (½ABq, J = 18 Hz, 4 H), 2.19 (s, 4 H) ppm. ^{13}C NMR (75 MHz, $CDCl_3$): δ = 122.4 (4 C), 59.7 (4 C), 36.0 (2 C), 31.3 (4 C) ppm. LRMS (ES, 70 eV): m/z = 239 [M + Na]$^+$. HRMS (ES): calcd. for $C_{14}H_{16}O_2Na$ [M + Na]$^+$ 239.1048; found 239.1052.

***syn*-Diepoxide:** M.p. 186.5–187.0 °C (dec.). ^{1}H NMR (300 MHz, $CDCl_3$): δ = 5.42 (s, 4 H), 2.57 (½ABq, J = 16 Hz, 4 H), 2.48 (½ABq, J = 16 Hz, 4 H), 2.24 (½ABq, J = 17 Hz, 2 H), 2.06 (½ABq, J = 18 Hz, 2 H) ppm. ^{13}C NMR (75 MHz, $CDCl_3$): δ = 122.1 (4 C), 58.4 (4 C), 33.4 (2 C), 31.1 (4 C) ppm. LRMS (ES, 70 eV): m/z = 239 [M + Na]$^+$. HRMS (ES): calcd. for $C_{14}H_{16}O_2Na$ [M + Na]$^+$ 239.1048; found 239.1056.

1,4,4a,5,8,8a,9,9a,10,10a-Decahydro-4a,8a,9a,10a-anthracenetetrol (16): There is a wide difference in the rates of hydrolysis of the two diepoxides. Thus, while the *syn* isomer undergoes complete hydrolysis in 10% aqueous acetic acid within 12 h at room temperature, the *anti* isomer under the same conditions reacts extremely slowly, with the reaction taking nearly 1.5 d to complete. Since both isomers gave the same tetrol **16**, the hydrolytic reaction was carried out with the mixture of the diepoxides **15**. A suspension of the mixture (200 mg, 0.926 mmol) in acetic acid (10% solution in water, 3 mL) was stirred vigorously at 50 °C for 6 h. The progress of the reaction was indicated by the slow conversion of the crystalline diepoxide into a voluminous white suspension. At the end of the reaction, the reaction mixture was cooled and the volatiles removed under vacuum to give the crude tetrol as a white powder. The crude compound was washed repeatedly with dichloromethane and then ethyl acetate to remove traces of the starting material. The tetrol thus obtained (221 mg, 95%) was sufficiently pure, as evident from its spectroscopic data, for use in further transformations. However further purification can be achieved by crystallization from methanol. M.p. 253.5–255.5 °C (dec.).[20] IR (KBr): $\tilde{\nu}$ = 3256, 3023, 1653 cm^{-1}. ^{1}H NMR (300 MHz, CD_3OD): δ = 5.55 (s, 4 H), 2.36 (½ABq, J = 17 Hz, 4 H), 2.06 (½ABq, J = 14 Hz, 2 H), 1.94 (½ABq, J = 17 Hz, 4 H), 1.46 (½ABq, J = 14 Hz, 2 H) ppm. ^{13}C NMR (75 MHz, CD_3OD): δ = 124.6 (4 C), 74.3 (4 C), 40.6 (2 C), 37.0 (4 C) ppm. LRMS (ES, 70 eV): m/z = 275 [M + Na]$^+$. HRMS (ES): calcd. for $C_{14}H_{20}O_4Na$ [M + Na]$^+$ 275.1259; found 275.1265.

Perhydro-4a,8a,9a,10a-anthracenetetrol (3): A heterogeneous mixture of the unsaturated tetrol **16** (100 mg, 0.397 mmol) and 5% Pd-C (10 mg, 10% w/w) in methanol (2 mL) was hydrogenated under 1 Torr pressure for 1 h. After the disappearance of the starting material, as indicated by TLC analysis, the reaction mixture was filtered through a small pad of Celite and washed with methanol. The combined filtrate and washings were concentrated under vacuum and the residue purified by column chromatography to afford **3** (96 mg, 95%) as a colorless, crystalline solid. M.p. 327.6–327.7 °C (dec.). IR (KBr): $\tilde{\nu}$ = 3275 cm^{-1}. ^{1}H NMR (300 MHz, 1:1 $CDCl_3$/CD_3OD): δ = 1.78 (½ABq, J = 15 Hz, 2 H), 1.66–1.58 (m, 4 H), 1.46–1.40 (m, 4 H), 1.22 (m, 4 H), 1.10–1.06 (m, 4 H), 0.935 (½ABq, J = 15 Hz, 2 H) ppm. ^{13}C NMR (75 MHz, $CDCl_3$): δ = 74.2 (4 C), 40.1 (2 C), 32.7 (4 C), 19.2 (4 C) ppm. LRMS (ES, 70 eV): m/z = 279 [M + Na]$^+$. HRMS (ES): calcd. for $C_{14}H_{24}O_4Na$ [M + Na]$^+$ 279.1272; found 279.1285.

Crystal Structure Analysis: The single-crystal X-ray diffraction data were collected with a Bruker AXS SMART APEX CCD diffractometer at 296 K. The X-ray generator was operated at 50 kV and 35 mA using Mo-K_α radiation. Crystal data for the polycyclitols **1**–**3** are given in Table 4. The data was collected with an ω scan width of 0.3°. A total of 606 frames per set were collected using SMART[21a] at three different settings of φ (0, 90 and 180°) or at four different settings of φ (0, 90, 180 and 270°) for triclinic crystal systems, keeping the sample-to-detector distance at 6.062 cm and the 2θ value fixed at –25°. All the data were corrected for Lorentzian, polarization and absorption effects using the SAINT[21b] and SADABS[22] programs. SHELX-97[23] was used for structure solution and full-matrix least-squares refinement on F^2. Hydrogen atoms were included in the refinement using the riding model. Details of the intra- and intermolecular hydrogen-bonding scheme were calculated using PARST95[24] and PLATON.[25]

CCDC-273131 (for tetrol **1**), -273132 (for hexol **2**), -250461 (for tetrol **3**) and -601706 (for diepoxide **12**) contain the supplementary crystallographic data for this paper. These data can be obtained free of charge from The Cambridge Crystallographic Data Centre via www.ccdc.cam.ac.uk/data_request/cif.

Table 4. Summary of the crystal data, data collection, structure solution, and refinement details for **1**–**3**.

	1	**2**	**3**
Formula	$C_{10}H_{18}O_4$	$C_{10}H_{18}O_6$	$C_{14}H_{24}O_4$
M_r	202.12	234.25	256.34
Crystal size [mm]	0.30 × 0.27 × 0.20	0.46 × 0.33 × 0.21	0.14 × 0.10 × 0.09
Crystal system	orthorhombic	monoclinic	triclinic
Space group	*Fdd2*	$P2_1/n$	$P\bar{1}$
a [Å]	20.432(5)	5.7859(12)	5.958(5)
b [Å]	17.320(7)	14.326(3)	5.994(5)
c [Å]	7.0558(17)	6.5982(14)	9.867(8)
α [°]	90	90	86.177(13)
β [°]	90	106.683(3)	82.547(13)
γ [°]	90	90	73.200(12)
V [Å^3]	3938.6(17)	523.90(19)	334.3(5)
Z	16	2	1
F (000)	1760	252	140
$\rho_{calcd.}$ [g cm^{-3}]	1.364	1.485	1.273
μ [mm^{-1}]	0.104	0.123	0.092
Absorption correction	multiscan	multiscan	multiscan
Min./max. transmission	0.9694/0.9795	0.9387/0.9747	0.9620/0.9918
Reflrctions collected	7591	3785	2431
No. of l.s. parameters	131	76	84
Unique reflections	1090	960	1213
Observed reflections	999	894	1038
Index range	$-25 \le h \le 25$ $-33 \le k \le 33$ $-8 \le l \le 8$	$-7 \le h \le 7$ $-15 \le k \le 17$ $-7 \le l \le 7$	$-7 \le h \le 7$ $-6 \le k \le 7$ $-11 \le l \le 11$
R_1 [$I > 2\sigma(I)$]	0.0426	0.0379	0.0504
wR_2	0.0914	0.1160	0.1405
Goodness of fit	1.331	1.023	1.058
$\Delta\rho_{max/min}$ [e Å^{-3}]	0.303/–0.220	0.284/–0.188	0.315/–0.203

Acknowledgments

We thank Prof. K. Venkatesan for his critical comments and helpful advice in preparing the manuscript and DST, India for the CCD facility at IISc, Bangalore.

[1] a) C. B. Aakeröy, K. R. Seddon, *Chem. Soc. Rev.* **1993**, *22*, 397–407; b) G. R. Desiraju, *Angew. Chem. Int. Ed. Engl.* **1995**, *34*, 2311–2327; G. R. Desiraju, *Angew. Chem.* **1995**, *107*, 2541–2558; c) G. R. Desiraju, *Crystal engineering. The design of organic solids*; Elsevier, Amsterdam, **1989**; d) C. B. Aakeröy, *Acta Crystallogr., Sect. B* **1997**, *53*, 569–586.

[2] For some selected recent references on crystal engineering and its applications, see: a) C. B. Aakeröy, A. M. Beatty, *Aust. J. Chem.* **2001**, *54*, 409–421; b) M. D. Hollingsworth, *Science* **2002**, *295*, 2410–2413; c) O. Almarsson, M. J. Zaworotko, *Chem. Commun.* **2003**, 1889–1896; d) D. Braga, *Chem. Commun.* **2003**, 2751–2754; e) B. Kojić-Prodić, Z. Štefanić, M. Žinić, *Croat. Chem. Acta* **2004**, *77*, 415–425; f) P. Erk, H. Hengelsberg, M. F. Haddow, R. van Gelder, *CrystEngComm* **2004**, *6*, 474–483; g) M. D. Ward, M. J. Horner, *CrystEngComm* **2004**, *6*, 401–407; h) S. George, A. Nangia, C.-K. Lam, T. C. W. Mak, J.-F. Nicoud, *Chem. Commun.* **2004**, *21*, 1202–1203; i) D. Schlatter, R. Thoma, E. Kueng, M. Stihle, F. Mueller, E. Borroni, A. Cesura, M. Hennig, *Acta Crystallogr., Sect. D* **2005**, *61*, 513–519; j) K. Kinbara, *Synlett* **2005**, 732–743; k) A. V. Trask, W. D. S. Motherwell, W. Jones, *Cryst. Growth Des.* **2005**, *5*, 1013–1021.

[3] a) G. A. Jeffrey, *Acta Crystallogr., Sect. B* **1990**, *46*, 89–103; b) G. A. Jeffrey, W. Saenger, *Hydrogen bonding in biological structures*, Springer, Berlin, **1991**; c) C. André, P. Lurger, J.-H. Fuhrhop, B. Rosengarten, *Acta Crystallogr., Sect. B* **1993**, *49*, 375–382; d) G. A. Jeffrey, *An Introduction to Hydrogen Bonding*; Oxford University Press, Oxford, **1997**; e) A. Bonnet, J. Chisholm, W. D. S. Motherwell, W. Jones, *CrystEngComm* **2005**, *7*, 71–75.

[4] R. Taylor, C. F. Macrae, *Acta Crystallogr., Sect. B* **2001**, *57*, 815–827.

[5] C. P. Brock, *Acta Crystallogr., Sect. B* **2002**, *58*, 1025–1031.

[6] V. T. Nguyen, P. D. Ahn, R. Bishop, M. L. Scudder, D. C. Craig, *Eur. J. Org. Chem.* **2001**, 4489–4499.

[7] The term "polycyclitol" is derived from "polycyclic cyclitols", and as the name suggests, refers to any polyhydroxylated molecule consisting of one or more cyclitol units embedded in a polycyclic carbon framework; see: a) G. Mehta, S. S. Ramesh, *Chem. Commun.* **2000**, 2429–2430; b) G. Mehta, S. S. Ramesh, *Tetrahedron Lett.* **2001**, *42*, 1987–1990.

[8] a) G. Mehta, S. Sen, K. Venkatesan, *CrystEngComm* **2005**, *7*, 398–401; b) G. Mehta, S. Sen, S. S. Ramesh, *CrystEngComm* **2005**, *7*, 563–568; c) G. Mehta, S. Sen, *CrystEngComm* **2005**, *7*, 656–663.

[9] a) G. Mehta, S. S. Ramesh, M. K. Bera, *Chem. Eur. J.* **2003**, *9*, 2264–2272; b) G. Mehta, S. S. Ramesh, *Tetrahedron Lett.* **2003**, *44*, 3105–3108; c) G. Mehta, S. S. Ramesh, *Eur. J. Org. Chem.* **2005**, 2225–2238.

[10] The details of the synthetic procedures followed in the preparation of the polycyclitols **1**–**3** have been included in the Exp. Sect.

[11] A. Shani, F. Sondheimer, *J. Am. Chem. Soc.* **1967**, *89*, 6310–6317.

[12] Crystal data for **12**: $C_{10}H_{14}O_4$, M = 252.31, monoclinic, space group $P2_1/n$, a = 6.557(1), b = 6.240(1), c = 10.861(2) Å, β = 90.319(3)°, V = 444.40(2) Å^3, Z = 2, F(000) = 212, $\rho_{calcd.}$ = 1.48 g cm^{-3}, μ = 0.114 mm^{-1}, T = 293 K, R_1 = 0.045, wR_2 = 0.103, GOF = 1.118 for 724 reflections with $I > 2\sigma(I)$. An ORTEP plot of **12**, with displacement ellipsoids for non-hydrogen atoms drawn at the 50% probability level, is shown below.

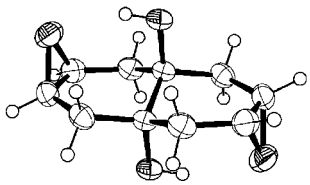

[13] a) A. J. Birch, P. Fitton, D. C. C. Smith, D. E. Steere, A. R. Stelfox, *J. Chem. Soc.* **1963**, 2209–2216; b) J. J. Runge, *Prakt. Chem.* **1966**, *31*, 280–292; c) R. G. Harvey, *J. Org. Chem.* **1967**, *32*, 238–240.
[14] a) E. Vogel, M. Biskup, A. Vogel, H. Günther, *Angew. Chem. Int. Ed. Engl.* **1973**, *12*, 989–991; b) E. Vogel, F. Kuebart, J. A. Marco, R. Andree, *J. Am. Chem. Soc.* **1983**, *105*, 6982–6983; c) P. J. Garatt, F. Sondheimer, *J. Chem. Soc., C* **1967**, 565–568.
[15] a) T. W. Craig, G. R. Harvey, G. A. Berchtold, *J. Org. Chem.* **1967**, *32*, 3743–3749; b) G. Mehta, S. Sen, S. Dey, *Acta Crystallogr., Sect. C* **2005**, *61*, o358–360.
[16] a) C. P. Brock, B. Schweizer, J. D. Dunitz, *J. Am. Chem. Soc.* **1991**, *113*, 9811–9820; b) M. C. Etter, K.-S. Huang, *Chem. Mater.* **1992**, *4*, 824–827; c) A. Gavezzotti, *Synlett* **2002**, 201–214; d) M. S. Hendi, P. Hooter, R. E. Davis, V. M. Lynch, K. A. Wheeler, *Cryst. Growth Des.* **2004**, *4*, 95–101.
[17] C. P. Brock, J. D. Dunitz, *Chem. Mater.* **1994**, *6*, 1118–1127.
[18] Owing to the absence of any significant anomalous scatterers (Z > Si), attempts to confirm the absolute structure by refinement of the Flack parameter led to an inconclusive value of 0.4(16) (see ref.[19]). Therefore the intensities of the Friedel pairs (883) were averaged prior to merging of data in *Fdd2* and the absolute configuration was assigned arbitrarily. The reported value of R_{int} corresponds to subsequent merging of equivalent reflections in this space group.
[19] a) H. D. Flack, *Acta Crystallogr., Sect. A* **1983**, *39*, 876–888; b) H. D. Flack, G. Bernardinelli, *J. Appl. Crystallogr.* **2000**, *33*, 1143–1148.
[20] The tetrol **16** crystallizes from methanol in two concomitant polymorphic modifications (see ref.[8a]). The melting point reported corresponds to that of the major polymorph of the tetrol.
[21] a) *SMART* (V6.028), Bruker AXS Inc., Madison, Wisconsin, USA, **1998**; b) *SAINT* (V6.02), Bruker AXS Inc., Madison, Wisconsin, USA, **1998**.
[22] G. M. Sheldrick, *SADABS*, University of Göttingen, Germany, **1996**.
[23] G. M. Sheldrick, *SHELXL97*, University of Göttingen, Germany, **1997**.
[24] M. Nardelli, *J. Appl. Crystallogr.* **1995**, *28*, 659.
[25] A. L. Spek, *Acta Crystallogr., Sect. A* **1990**, *46*, C34.

Received: July 17, 2006
Published Online: October 18, 2006

